

## Photoinduced Electron Transfer between Fluorescent Dyes and Guanosine Residues in DNA-Hairpins

Thomas Heinlein, Jens-Peter Knemeyer, Oliver Piestert, and Markus Sauer\*

Physikalisch-Chemisches Institut, Universität Heidelberg, Im Neuenheimer Feld 253, 69120 Heidelberg, Germany

Received: March 28, 2003; In Final Form: May 19, 2003

Nucleobase-specific quenching interactions of fluorescent dyes can be used in singly labeled hairpin-shaped oligonucleotides to detect hybridization to specific target DNA sequences. In these DNA-hairpins, the dye is attached at the 5'-end and quenched by guanosine residues in the complementary stem. Upon hybridization, a conformational reorganization occurs reflected in an increase in fluorescence intensity. To gain a better insight into the underlying quenching mechanism, we have performed intermolecular quenching experiments with different dyes (rhodamine and oxazine derivatives) and DNA nucleotides. The bimolecular dynamic quenching rate constants  $k_{q,dyn}$  of  $\sim 1.0\text{--}2.0 \times 10^9 \text{ M}^{-1} \text{ s}^{-1}$  are relatively small for all dyes investigated though the measured decrease in fluorescence intensity indicates strong static fluorescence quenching. The data give evidence for the formation of weak or nonfluorescent (fluorescence lifetime,  $\tau < 40$  ps) ground-state complexes between the fluorophores and guanosine residues. Only within these complexes, that is, upon contact formation, efficient fluorescence quenching via electron transfer occurs. Using a model DNA-hairpin labeled at the 5'-end with the oxazine derivative MR121, we varied the position of guanosine in the complementary stem sequence to reveal the distance dependence of fluorescence quenching. Qualitatively, it is apparent that the double-stranded stem of the DNA-hairpin facilitates efficient electron transfer from the guanosine residue to MR121 with a shallow distance dependence. This result strongly supports the idea that an end-capped conformation with stacking interactions and subsequent DNA mediated electron transfer is required for efficient fluorescence quenching. Our data show that the quenching efficiency can be increased substantially by the attachment of additional overhanging single-stranded nucleotides at the 3'-end and the substitution of guanosine by stronger electron-donating nucleotides, such as 7-deazaguanosine residues. Consideration of the data obtained in this study enables the synthesis of DNA-hairpins solely quenched by guanosine residues and its analogous with a 20-fold increase in fluorescence intensity upon specific binding to the target sequence.

### Introduction

The understanding of specific and nonspecific interactions between fluorescent dyes and DNA bases are increasingly important for the development of new efficient and highly sensitive *in vitro* and *in vivo* DNA or RNA detection schemes. Within recent years, several fluorescence-based hybridization assays for the quantification of specific DNA or RNA molecules in homogeneous solution have been proposed.<sup>1–6</sup> Most methods incorporate the use of an oligonucleotide labeled with a donor (D) and an acceptor fluorophore (A) or a quencher (Q) to quantitatively determine the amount of specific target sequence synthesized during polymerase chain reaction (PCR). Using fluorescence resonance energy transfer (FRET), the fluorescence of D is quenched by the presence of A via dipole–dipole interactions.<sup>7</sup> Förster type resonant energy transfer occurs for allowed singlet–singlet transitions if the emission of D and the absorption of A overlap significantly. For such transitions, the critical transfer radii range from 20 to 80 Å.<sup>8</sup> Electronic interactions between a fluorophore and a quencher (Q) usually occur in the strong coupling range, that is, at distances between D and Q below 2 nm.<sup>9</sup> The separation of D and A or Q occurs either by cleavage of the oligonucleotide or by a change in

secondary structure of the oligonucleotide probe when it anneals to target DNA or RNA.

A conformational change upon hybridization constitutes the basis of the “molecular beacon” technology.<sup>10–12</sup> A molecular beacon consists of a single-stranded DNA molecule in a stem-loop conformation with a donor fluorophore linked to the 5' position and a quencher, for example, 4-((4-(dimethylamino)phenyl)azo)benzoic acid (DABCYL), at the 3' terminus. In the hybridized form, the stem holds Q and D in close proximity to each other; consequently, the donor dye is quenched efficiently via dipole–dipole or electronic interactions as long as the stem-loop structure exists. Upon specific hybridization of the loop with a target sequence, the stem is forced apart, leading to a spatial separation of D and Q. Typically, the fluorescence intensity of D increases  $\sim 10\text{--}40$  fold upon specific hybridization to the target sequence. Since molecular beacons are remarkably effective at detecting single-base mismatches, they hold great promise for studies in genetics, disease mechanisms, and molecular interactions.<sup>10–12</sup>

However, molecular beacons have important limitations. First, they require site-specific labeling of the DNA-hairpin with two extrinsic probes, a donor and a quencher dye. Production of oligonucleotides with dual modifications is still relatively expensive. A method that takes advantage of properties of

\* To whom correspondence should be addressed. Phone: +49-6221-548460; fax: +49-6221-544255; e-mail: sauer@urz.uni-heidelberg.de.

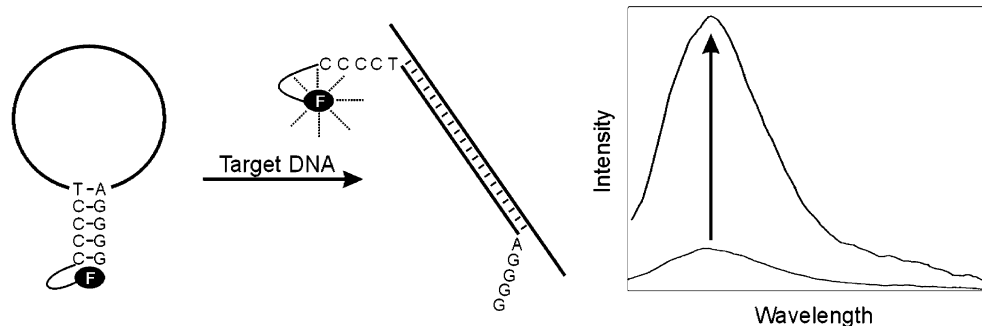


**Figure 1.** Schematic of operation of singly labeled DNA-hairpins. The fluorophore is attached to the 5'-end of the oligonucleotide and quenched by guanosine residues in the complementary stem via photoinduced intramolecular electron transfer. Upon hybridization to the target sequence (complementary to the loop sequence), the fluorescence is restored because of a conformational reorganization that forces the stem apart.

naturally occurring nucleotides would be more useful. Second, since the two termini of the DNA-hairpin are already occupied by the donor and acceptor, respectively, further modification of such an oligonucleotide, for example, to attach it to a solid support via biotin/streptavidin binding, requires the incorporation of amino-modified or biotinylated nucleotides into the stem.<sup>13</sup> Instead of using interactions between two extrinsic probes, interactions of fluorophores with DNA bases or amino acids can be used for the specific detection of DNA or RNA sequences and antibodies at the single-molecule level.<sup>14,15</sup> Nucleobase-specific interactions have been reported for rhodamine,<sup>16–18</sup> oxazine,<sup>19</sup> fluorescein,<sup>20,21</sup> Bodipy-FL,<sup>22</sup> pyrene,<sup>23,24</sup> stilbene,<sup>25</sup> and coumarin dyes.<sup>26</sup>

Recently, we introduced a novel method to synthesize DNA-hairpins that takes advantage of the fact that several fluorophores are selectively quenched by guanosine residues (Figure 1).<sup>27</sup> The method uses the differences in specific properties of naturally occurring nucleotides, in particular, the low oxidation potential of the DNA base guanosine<sup>26,28</sup> and the tendency of many fluorophores to aggregate in aqueous environment to decrease their water accessible area. Thus, dependent on the reduction potential of the fluorophore used to label the DNA-hairpin, efficient photoinduced intramolecular electron transfer (PET) occurs in the excited state upon contact formation with guanosine. In contrast to electronic energy transfer based systems where long-range dipole–dipole interactions occur, these sensors require close contact between the fluorophore and the guanosine or tryptophan residue for efficient PET. With careful design of these conformationally flexible probes and the use of appropriate fluorophores (rhodamine and oxazine dyes are well suited candidates), efficient single-molecule sensitive DNA-hairpins can be produced.<sup>27</sup> If quenching interactions between the fluorophore and the guanosine residue are deteriorated upon specific binding to the target, for example, because of binding of a complementary DNA sequence or because of cleavage by an endonuclease enzyme, fluorescence of the DNA-hairpin is restored (Figure 1). DNA-hairpins labeled with a single oxazine dye at the 5'-end increase fluorescence upon hybridization 6-fold,<sup>27</sup> which may provide a basis for a cost-effective and highly sensitive DNA/RNA detection method. Very recently,<sup>29</sup> immobilized DNA-hairpins based on nucleobase-specific fluorescence quenching of an oxazine dye have been used successfully to detect the presence of sub-picomolar target DNA sequence. Therefore, they offer an elegant alternative to conventional molecular beacons based on electronic energy transfer processes.

In this paper, we demonstrate that by the appropriate design of singly labeled DNA-hairpins an increase in fluorescence intensity of >20-fold upon hybridization to the target sequence

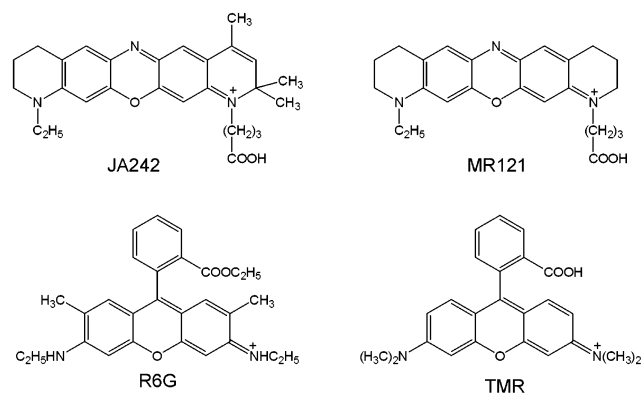


**Figure 2.** Molecular structures of the fluorophores MR121, JA242, rhodamine 6G (R6G), and tetramethylrhodamine (TMR) investigated in intermolecular quenching experiments.

can be realized. This has been achieved by a careful study of different factors that influence the photoinduced intramolecular electron transfer efficiency. Among these are the selection of suitable fluorophores, the influence of the guanosine position in the complementary stem, the attachment of additional overhanging single-stranded nucleotides in the complementary stem, and the exchange of guanosine by more potent electron donors, such as 7-deazaguanosine. Our data suggest that the fluorophore has to adopt an end-capped conformation with respect to the stem of the hairpin to ensure efficient electron transfer with guanosine residues. This end-capped conformation is stabilized by additional nucleotides attached at the end of the complementary stem sequence. The shallow distance dependence of charge transfer strongly suggest that only within the end-capped conformation efficient DNA-mediated electron transfer occurs.

## Experimental Section

**Materials.** The molecular structures of the fluorescent dyes are shown in Figure 2. MR121, JA242, and JA243 were kindly provided by K. H. Drexhage (Universität-Gesamthochschule Siegen, Germany), tetramethylrhodamine (TMR) and rhodamine 6G (R6G) were purchased from Molecular Probes (Göttingen, Germany). 2'-Deoxynucleosides (dNMPs) were used as received from Sigma. Oligonucleotides carrying a 5'-amino C6 modifier (Table 1) for covalent coupling of the dyes and complementary oligonucleotides were custom-synthesized by MWG-Biotech (Ebersberg, Germany).

**Synthesis of DNA-Hairpins.** 5'-end labeling of the oligonucleotides with the fluorescent oxazine dye MR121 was performed by classical N-hydroxysuccinimidylester (NHS-ester) chemistry using standard solvents purchased from Merck

**TABLE 1: Spectroscopic Characteristics and Bimolecular Quenching Constants for dGMP<sup>a</sup>**

	$\lambda_{\text{abs}}$ (nm)	$\lambda_{\text{em}}$ (nm)	$\tau_1$ (ns)	$\tau_2$ (ns)	$a_1$	$a_2$	$K_{\text{as}}$ (M <sup>-1</sup> )	$k_{\text{q,s}}$ ( $\times 10^9$ M <sup>-1</sup> s <sup>-1</sup> )	$k_{\text{q,dyn}}$ ( $\times 10^9$ M <sup>-1</sup> s <sup>-1</sup> )
MR121	661	673	1.85	1.00					
MR121/50 mM dGMP	666	674	1.54	0.79	0.12	0.21	120	64.8	2.00
JA242	664	682	1.89	1.00					
JA242/50 mM dGMP	668	683	1.62	0.84	0.15	0.16	98	52.2	1.32
R6G	526	556	3.96	1.00					
R6G/50 mM dGMP	531	557	2.88	0.68	0.31	0.32	182	46.1	2.08
TMR	551	581	2.25	1.00					
TMR/50 mM dGMP	556	583	1.85	0.63	0.21	0.37	50	22.6	1.81

Absorption maxima ( $\lambda_{\text{abs}}$ ), emission maxima ( $\lambda_{\text{em}}$ ), and fluorescence lifetimes ( $\tau$ ) of  $10^{-7}$  M solutions of the rhodamine derivatives rhodamine 6G (R6G) and tetramethylrhodamine (TMR) and the oxazine derivatives MR121 and JA242 in the absence and presence of 50 mM dGMP in PBS buffer, pH 7.4, containing 5 mM MgCl<sub>2</sub>. Fluorescence lifetimes were measured at the emission maxima ( $\chi^2 = 0.90\text{--}1.15$ ). In addition, the bimolecular static and dynamic quenching constants  $k_{\text{q,s}}$  and  $k_{\text{q,dyn}}$ , respectively, and association constants,  $K_{\text{as}}$  are given (3 $\sigma$ -error estimation: 10% for  $k_{\text{q,s}}$  and  $k_{\text{q,dyn}}$ ).  $k_{\text{q,s}}$  was determined from the linear area of the static bimolecular Stern–Volmer plots (0–20 mM dGMP).  $k_{\text{q,dyn}}$  was determined from the longer, quencher-dependent fluorescence lifetime,  $\tau_1$ .

(Darmstadt, Germany). To one mole equivalent of oligonucleotide a 5-fold excess of activated dye was added, dissolved in 0.1 M carbonate buffer (pH 9.4), and stirred for 6 h in the dark. Labeled oligonucleotides were purified by HPLC (Hewlett-Packard, Böblingen, Germany) using a reversed-phase column (Knauer, Berlin, Germany) with octadecylsilan-hypersil C18. Separation was performed in 0.1 M triethylammonium acetate, using a linear gradient from 0 to 75% acetonitrile in 20 min. Reaction yields of the 5'-end labeled products of up to 85% were obtained. Purity of the probes was checked by capillary gel electrophoresis.

**Absorption and Fluorescence Spectroscopy.** All measurements were carried out at room temperature (25 °C) in PBS buffer, pH 7.4, containing 5 mM MgCl<sub>2</sub>. Absorption spectra were taken on a Cary 500 UV–vis–NIR spectrometer (Varian, Darmstadt, Germany). Steady-state fluorescence spectra were measured in standard quartz cuvettes with a LS100 spectrometer (Photon Technology International, Wedel, Germany). Corrected fluorescence spectra were obtained using a high-pressure xenon flash lamp as excitation source. To avoid reabsorption and re-emission effects, concentrations were kept strictly below 1  $\mu\text{M}$  (typically 0.1  $\mu\text{M}$ ) in all measurements. Ensemble fluorescence lifetime measurements were performed on a 5000MC spectrometer (IBH, Glasgow, United Kingdom) using the time-correlated single-photon-counting (TCSPC) technique. As excitation source a pulsed laser diode with a repetition rate of 1 MHz and a pulse length of  $\sim 200$  ps (fwhm) or a light-emitting diode (center 495 nm) with a repetition rate of 1 MHz and a pulse length of  $\sim 1$  ns (fwhm) was used. With this setup, instrument response functions (IRF) of 220 ps and 1 ns (fwhm) were measured. To exclude polarization effects, fluorescence was observed under magic angle (54.7°) conditions. Typically, 5000 photon counts were collected in the maximum channel using 2056 channels. The decay parameters were determined by least-squares deconvolution, and their quality was judged by the reduced  $\chi^2$  values and the randomness of the weighted residuals. In the case that a monoexponential model was not adequate to describe the measured decay, a multiexponential

model was used to fit the decay (eq 1),

$$I(t) = I(0) \sum a_i \tau_i \quad (1)$$

where  $a_i$  are the preexponential factors that describe the ratio of the excited species and  $\tau_i$  denote their lifetimes. Fluorescence anisotropies at the emission maxima,  $r$ , for the dyes were calculated from the polarization of the emission components,  $I_{\text{VV}}$ ,  $I_{\text{VH}}$ ,  $I_{\text{HV}}$ , and  $I_{\text{HH}}$  (where the subscripts denote the orientation of the excitation and emission polarizers) as (eq 2)

$$r = \frac{(I_{\text{VV}} - GI_{\text{VH}})}{(I_{\text{VV}} + GI_{\text{VH}})} \quad (2)$$

where  $G = I_{\text{HV}}/I_{\text{HH}}$ .

## Results and Discussion

**Intermolecular Fluorescence Quenching Experiments.** To interpret quenching efficiencies of DNA nucleotides and fluorophores, bimolecular quenching experiments with two rhodamine (R6G, TMR) and two oxazine derivatives (MR121, JA242) were performed with deoxynucleotide monophosphates (dNMPs). Bimolecular static and dynamic quenching constants,  $k_{\text{q,s}}$  and  $k_{\text{q,dyn}}$ , were determined from steady-state and time-resolved fluorescence quenching experiments using Stern–Volmer analysis (eq 3 and 4),

$$F_0/F = 1 + K_s[\text{Q}] = 1 + k_{\text{q,s}}\tau_0[\text{Q}] \quad (3)$$

$$\tau_0/\tau = 1 + K_{\text{dyn}}[\text{Q}] = 1 + k_{\text{q,dyn}}\tau_0[\text{Q}] \quad (4)$$

where  $\tau_0$  and  $F_0$  are the fluorescence lifetime and intensity in the absence of a quencher,  $\tau$  and  $F$  are the fluorescence lifetime and intensity in the presence of the quencher Q with the concentration [Q], and  $K_s$  and  $K_{\text{dyn}}$  denote the static and dynamic Stern–Volmer constant, respectively. Among the four DNA bases only dGMP quenches the fluorescence of rhodamine and oxazine dyes significantly with bimolecular static quenching constants,  $k_{\text{q,s}}$ , of  $20\text{--}65 \times 10^9 \text{ M}^{-1} \text{ s}^{-1}$  (Figure 3A, Table 1). The bimolecular static quenching constants,  $k_{\text{q,s}}$ , for dGMP calculated from the linear region of the Stern–Volmer plots are summarized in Table 1. Only the oxazine derivative MR121 is additionally quenched by dAMP reflected in a comparably small bimolecular static quenching constant,  $k_{\text{q,s}}$ , of  $5.9 \times 10^9 \text{ M}^{-1} \text{ s}^{-1}$ . The quenching experiments yielded identical results, within error, in phosphate-buffered saline (PBS) pH 7.4, 5 mM MgCl<sub>2</sub>, and unbuffered H<sub>2</sub>O. In addition, the absorption maxima of all four dyes investigated show bathochromic shifts of 4–6 nm upon addition of deoxynucleotide monophosphates (dNMPs). The emission maxima are only slightly shifted toward the red indicating the formation of non- or only weakly fluorescent ground-state complexes. As can be seen in Figure 3A, Stern–Volmer plots obtained from steady-state measurements display upward curvatures for the two oxazine derivatives MR121 and JA242 and a downward curvature for the rhodamine derivative R6G. These deviations from linearity at higher quencher concentrations indicate the existence of at least two populations of fluorophores: the formation of nonfluorescent ground-state complexes between the oxazine derivatives and dGMP and the formation of weakly fluorescent complexes between R6G and dGMP resulting in upward and downward curvatures, respectively, at higher quencher concentrations. Comparison of the bimolecular static quenching constants,  $k_{\text{q,s}}$ , of  $20\text{--}65 \times 10^9 \text{ M}^{-1} \text{ s}^{-1}$  (Table 1) with the estimated diffusion-

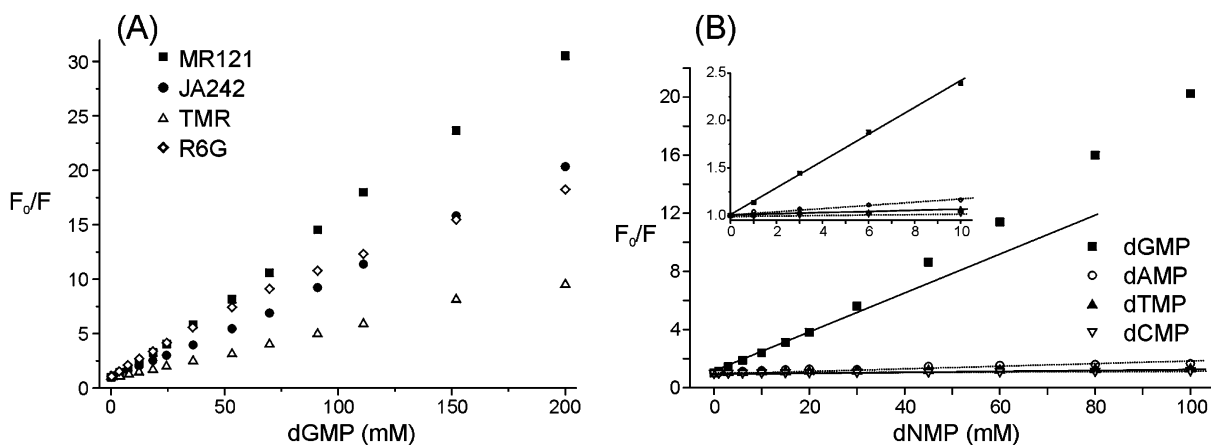


**Figure 3.** (A) Static bimolecular Stern–Volmer plots of the oxazine derivatives MR121 and JA242 and the rhodamine derivatives tetramethylrhodamine (TMR) and rhodamine 6G (R6G) with guanosine monophosphate (dGMP) in PBS buffer, pH 7.4, containing 5 mM MgCl<sub>2</sub>. (B) Static bimolecular Stern–Volmer plots of MR121 and the four DNA monophosphates dGMP, dAMP, dTMP, and dCMP in PBS buffer, pH 7.4, containing 5 mM MgCl<sub>2</sub>. The inset shows an expanded view of the linear area of the static Stern–Volmer plot.

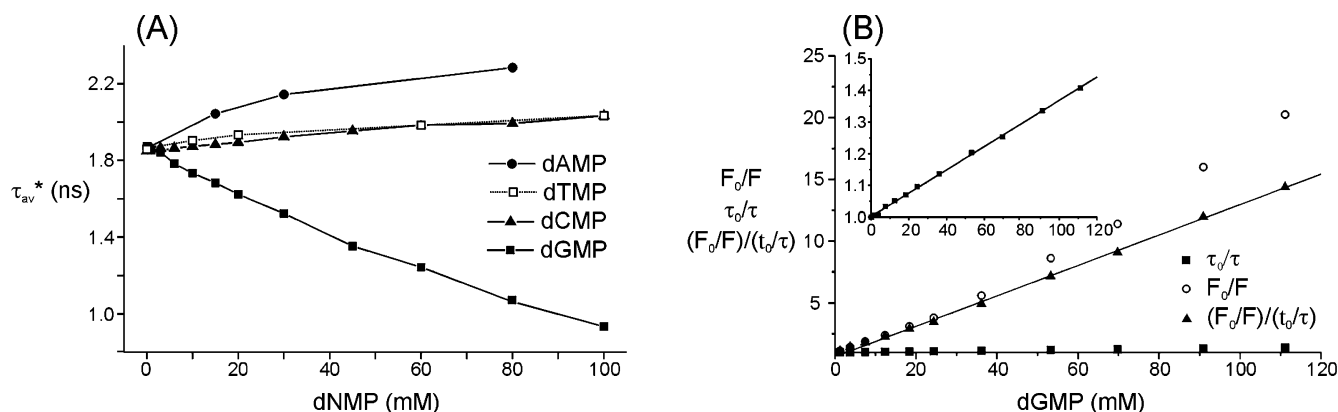


**Figure 4.** (A) Average fluorescence lifetime,  $\tau_{av}^* = \sum a_i \tau_i$ , of MR121 in PBS buffer, pH 7.4, containing 5 mM MgCl<sub>2</sub> with increasing concentration of dNMPs. The fluorescence lifetimes increase upon addition of dAMP, dCMP, and dTMP but decrease as a result of quenching electron transfer in the presence of dGMP. (B) Static and dynamic bimolecular Stern–Volmer plots of MR121 and dGMP in PBS buffer, pH 7.4, containing 5 mM MgCl<sub>2</sub>. The inset shows an expanded view of the dynamic Stern–Volmer plot calculated from the longer, quencher-dependent fluorescence lifetime,  $\tau_1$ . Under the assumption that the ground-state complexes can be considered as essentially nonfluorescent, association constants,  $K_{as}$ , for the oxazine derivatives can be calculated via eq 5.  $K_{as}$  for R6G and TMR were calculated from the linear area of the static Stern–Volmer plots (0–20 mM).

controlled bimolecular constant of  $\sim 6.5 \times 10^9 \text{ M}^{-1} \text{ s}^{-1}$  supports the idea of the formation of non- or only weakly fluorescent ground-state complexes between the fluorophores and dGMP in aqueous solutions.

Time-resolved fluorescence quenching experiments with dGMP support the idea of the formation of non- or only weakly fluorescent ground-state complexes between rhodamine and oxazine derivatives in aqueous solvents. The fluorescence decays of the oxazine derivatives remain almost monoexponential with a long lifetime,  $\tau_1$ , dependent on the quencher concentration, and an additional shorter decay component of  $\sim 100$  ps for MR121 and  $\sim 150$  ps for JA242, independent of the dGMP concentration (Table 1). Only the amplitudes of the short decay time components,  $\tau_2$ , increase with increasing quencher concentration. The rhodamine dyes R6G and TMR show more pronounced multiexponential behavior in the presence of dGMP with short lifetime components of  $\sim 300$  and  $\sim 200$  ps independent of the dGMP concentration. Therefore, bimolecular dynamic quenching constants,  $k_{q,dyn}$ , were calculated from the longer, quencher concentration dependent lifetime,  $\tau_1$  (Table 1). The absolute values of fluorescence decay times of extremely short components ( $< 300$  ps) and their corresponding amplitudes determined from multiexponential decays are less reliable than the values of the longer decay times. Nevertheless, the data

demonstrate that the quencher concentration independent fluorescence decay times are shorter for oxazine derivatives.

Addition of dAMP, dTMP, or dCMP causes an increase in the fluorescence lifetime of all dyes investigated in aqueous surroundings (Figure 4A). These results evidence the formation of ground-state complexes between rhodamine and oxazine derivatives and DNA nucleotides in aqueous solvents. In case of association with guanosine nucleotides, fluorescence is efficiently quenched. The strong difference between the static and dynamic bimolecular quenching constants point out that efficient quenching occurs only in these complexes, that is, at van der Waals contact ( $\sim 0.4$  nm). The fact that the strong static quenching efficiency is not reflected in a reduction of the fluorescence lifetimes, especially for the two oxazine derivatives, indicates that they exhibit a fluorescence lifetime shorter than the time resolution of the instrument ( $\sim 40$  ps for excitation with the pulsed laser diode at 635 nm) used to measure the fluorescence decays. For example, the amplitude of the short constant lifetime  $a_2$  of  $\sim 0.1$ – $0.2$  at a dGMP concentration of 50 mM (Table 1) cannot account for the strong decrease in fluorescence intensity observed in static quenching experiments (Figure 3A). Therefore, dependent on the relative conformations and resulting interaction geometries, the complexes can be considered as essentially nonfluorescent. Then, the association

constant,  $K_{\text{as}}$ , can be calculated via eq 5 by plotting  $(F_0/F)/(\tau_0/\tau)$  versus the quencher concentration (Figure 4B).

$$F_0/F = (1 + K_{\text{dyn}}[Q])(1 + K_{\text{as}}[Q]) \quad (5)$$

As can be seen in Table 1, among the four dyes investigated R6G exhibits the highest association constant of  $K_{\text{as}} = 182 \text{ M}^{-1}$  with dGMP.<sup>18</sup> On the other hand, the oxazine derivative MR121 shows the most pronounced quenching efficiency.

**Mechanism of Fluorescence Quenching.** Intermolecular quenching experiments indicate that the underlying quenching mechanism is highly efficient only at short distances, that is, within the ground-state complexes. This is corroborated by the observation that the static quenching rate,  $k_{\text{q,s}}$ , strongly decreases upon addition of denaturing agents such as urea or guanidium chloride. Therefore, it can be concluded that hydrophobic interactions between the rhodamine and oxazine dyes and DNA nucleotides play an important role in the formation of these nonfluorescent ground-state complexes.<sup>30,31</sup> Fluorescence experiments in D<sub>2</sub>O did not give any evidence for the involvement of hydrogen bonds in fluorescence quenching. As collisional quenching is comparably inefficient (Table 1), a stacked arrangement of the guanine base and the rhodamine, or oxazine ring system in the complex, appears to be responsible for ultrafast fluorescence quenching.<sup>32,33</sup> Most likely, the mechanism involves a photoinduced electron-transfer interaction between guanine and the fluorophores. Photoinduced electron transfer (PET) from the DNA base guanine to excited rhodamine, oxazine, or stilbene dyes is a well known process.<sup>16–18,26,34,35</sup> Quenching of singlet rhodamine or oxazine dyes by guanine but not cytosine, thymine, or adenine nucleotides is consistent with a PET mechanism for fluorescence quenching in which the excited fluorophores serve as electron acceptors and guanine as a ground-state electron donor. PET reactions are controlled by the relation between the free energy of the reaction, the reorganization energy, and the distance between the donor and acceptor.<sup>36,37</sup> Furthermore, electron-transfer reactions do not require intimate molecular contact and may well occur over larger distances, for example, through space or through bond by a superexchange mechanism.<sup>35,38</sup> To get an idea about the efficiency of photoinduced charge separation, the free-energy change for charge separation,  $\Delta G_{\text{cs}}$ , can be estimated by using Weller's equation (eq 6),<sup>36,39</sup>

$$\Delta G_{\text{cs}} = E_{\text{ox}} - E_{\text{red}} - E_{0,0} + C \quad (6)$$

where  $E_{\text{ox}}$  and  $E_{\text{red}}$  are the first one-electron oxidation of the donor and the first one-electron reduction potential of the acceptor in the solvent under consideration.  $E_{0,0}$  is the energy of the zero–zero transition to the lowest excited singlet state of the excited partner, and  $C$  is the solvent dependent Coulombic attraction energy. The value of  $C$  in moderately polar environment is sufficiently small that it can be neglected. Table 2 gives the one-electron redox potentials measured versus the saturated calomel electrode (SCE) and the corresponding transition energies of some dyes. Among the four DNA nucleosides, dG exhibits the most pronounced electron-donating properties. Although other nucleosides such as 7-deazaguanine and the amino acid tryptophan are more potent donors with oxidation potentials of  $\sim 0.80$ – $1.00 \text{ V}$  versus SCE at neutral pH,<sup>40–43</sup> the electron-donating properties of dG are sufficient to quench most known rhodamine and oxazine derivatives (Table 2). On the other hand, carbocyanine dyes such as Cy5 are not quenched by guanine via PET. Unfortunately, the reduction potentials,  $E_{\text{red}}$ , of the oxazine derivatives MR121 and JA242 are not

**TABLE 2: First One-Electron Oxidation and Reduction Potentials,  $E_{\text{ox}}$  and  $E_{\text{red}}$ , of Fluorescent Dyes R6G, MR121, JA242, Cy5, and the Deoxynucleosides dG, dA, dC, and dT in Acetonitrile and Corresponding Zero–Zero Transition Energies,  $E_{0,0}$ , of the Dyes. In Addition, the Free-Energy Change for Charge Separation,  $\Delta G_{\text{cs}}$ , in Acetonitrile (Reduction of Excited Dyes by dG) Are Given**

	$E_{\text{ox}}$ (V/SCE)	$E_{\text{red}}$ (V/SCE)	$E_{0,0}$ (eV)	$\Delta G_{\text{cs}}$ (eV)
R6G <sup>a</sup>	1.39	−0.95	2.27	−0.07
MR121/JA242 <sup>b</sup>	1.40	−0.50	1.90	−0.15
Cy5 <sup>a</sup>	0.82	−0.88	1.88	0.25
dG <sup>c</sup>	1.25	<−3.00		
dA <sup>c</sup>	1.72	−2.76		
dC <sup>c</sup>	1.90	−2.59		
dT <sup>c</sup>	1.87	−2.42		

<sup>a</sup> Data taken from literature.<sup>44</sup> <sup>b</sup> Values estimated from measured values for several, structural related red-absorbing rhodamine derivatives.<sup>45–47</sup> <sup>c</sup> Redox potentials for the nucleosides were taken from Seidel et al.<sup>26</sup>

available. However,  $E_{\text{red}}$  can be estimated roughly from measured values for several, structural related red-absorbing rhodamine derivatives to approximately  $-0.5 \text{ V}$  versus SCE.<sup>45–47</sup> With a zero–zero transition energy,  $E_{0,0}$ , of  $\sim 1.9 \text{ eV}$  for MR121, the free-energy change for charge transfer,  $\Delta G_{\text{cs}}$ , from the ground-state guanine to the excited oxazine chromophore at infinite separation can be estimated to approximately  $-0.15 \text{ eV}$ . These data demonstrate that the electron-transfer reaction between rhodamine or oxazine derivatives and guanine is slightly exergonic.

#### Intramolecular Fluorescence Quenching in DNA-Hairpins.

Table 3 shows the sequence of the DNA-hairpins synthesized to study the quenching efficiency of guanosine nucleotides. Four guanosine residues are located at the 3'-end and the fluorophore is attached to the 5'-end via a C<sub>6</sub>-carbon linker. Absorption and emission maxima show bathochromic shifts of a few nanometers similar to the shifts observed in intermolecular quenching experiments. Among the three dyes investigated, MR121 shows the strongest decrease in fluorescence intensity with a relative fluorescence quantum yield,  $\Phi_{\text{f,rel}}$ , of 0.20 for DNA-hairpins containing four guanosine residues in the complementary stem (compare R6G-SP-1, JA242-SP-1, and MR121-SP-1 in Table 4). As a result of weak fluorescence quenching of MR121 by adenine (Figure 3B), the fluorescence quantum yield of MR121 labeled DNA-hairpins is always lower than  $\Phi_{\text{f,rel}}$  of the free dye. For example, the DNA-hairpin MR121-SP-6 exhibits a relative fluorescence quantum yield,  $\Phi_{\text{f,rel}}$ , of 0.89 (Table 4). Comparison of the fluorescence quantum yields and lifetimes measured for both oxazine derivatives, MR121 and JA242, shows that the quenching electron-transfer reactions are mainly manifested in static quenching. This indicates that the quenching reaction is faster than the time scale measured by our apparatus ( $\sim 40 \text{ ps}$ ) corresponding to a charge separation constant,  $k_{\text{cs}} > 2 \times 10^{10} \text{ s}^{-1}$ . In contrast, the decrease in measurable fluorescence lifetimes for R6G completely account for the quenching of the rhodamine derivative by guanine, indicating that charge separation takes place on a slower time scale ( $k_{\text{cs}} \sim 10^9 \text{ s}^{-1}$ ).

The distance dependence of charge separation was examined in a series of MR121 labeled DNA-hairpins carrying only a single guanosine nucleotide in the complementary stem at various positions. Assuming a relatively fixed location in an end-capped conformation with nearly coplanar orientation of the oxazine derivative and the G:C base pairs, this corresponds to donor/acceptor distances ranging from 3.4 to 13.6 Å (Table 4; MR121-SP-2, MR121-SP-3, MR121-SP-4, and MR121-SP-5). As can be seen in Figure 5A and 5C, the fluorescence quantum yields increase only slightly with separation distance

**TABLE 3: Sequences of DNA-Hairpins<sup>a</sup>**

abbreviation	oligonucleotide sequence
R6G-SP-1	R6G-C <sub>6</sub> -5'- <b>CCCCTTAGTAGTTCCTCACAAAGGGG</b> -3'
JA242-SP-1	JA242-C <sub>6</sub> -5'- <b>CCCCTTAGTAGTTCCTCACAAAGGGG</b> -3'
MR121-SP-1	MR121-C <sub>6</sub> -5'- <b>CCCCTTAGTAGTTCCTCACAAAGGGG</b> -3'
MR121-SP-2	MR121-C <sub>6</sub> -5'- <b>CAATTTAGTAGTTCCTCACAAATTG</b> -3'
MR121-SP-3	MR121-C <sub>6</sub> -5'- <b>ACATTTAGTAGTTCCTCACAAATGT</b> -3'
MR121-SP-4	MR121-C <sub>6</sub> -5'- <b>AACTTTAGTAGTTCCTCACAAAGTT</b> -3'
MR121-SP-5	MR121-C <sub>6</sub> -5'- <b>AACTTTAGTAGTTCCTCACAAAGTTT</b> -3'
MR121-SP-6	MR121-C <sub>6</sub> -5'- <b>AAATTTAGTAGTTCCTCACAAATTT</b> -3'
MR121-SP-1-TTT	MR121-C <sub>6</sub> -5'- <b>CCCCTTAGTAGTTCCTCACAAAGGGGTTT</b> -3'
MR121-SP-1-GGG	MR121-C <sub>6</sub> -5'- <b>CCCCTTAGTAGTTCCTCACAAAGGGGGGG</b> -3'
MR121-SP-1*-TTT	MR121-C <sub>6</sub> -5'- <b>CCCCTTAGTAGTTCCTCACAAAGGGG</b> <sup>7</sup> TTT-3'
MR121-SP-1** <sup>7</sup> -TTT	MR121-C <sub>6</sub> -5'- <b>CCCCTTAGTAGTTCCTCACAAAGGG</b> <sup>7</sup> G <sup>7</sup> TTT-3'

Nucleotides forming the double-stranded stem are marked bold. SP: DNA-hairpins quenched solely by the DNA base guanine were recently introduced as Smart Probes (SP).<sup>27</sup> G:<sup>7</sup> 7-deazaguanosin.

**TABLE 4: Relative Fluorescence Quantum Yields ( $\Phi_{F,rel}$ ) and Lifetimes ( $\tau$ ) of DNA-Hairpins in PBS Buffer, pH 7.4, Containing 5 mM MgCl<sub>2</sub><sup>a</sup>**

	$\tau_1$ (ns)	$a_1$	$\tau_2$ (ns)	$a_2$	$\chi^2$	$\Phi_{f,rel}$
R6G-SP-1	4.38	0.42	0.74	0.58	1.075	0.49
JA242-SP-1	2.92	0.79	0.63	0.21	1.003	0.44
MR121-SP-1	2.67	0.78	0.46	0.22	1.004	0.20
MR121-SP-2	2.76	0.94	0.45	0.06	1.114	0.43
MR121-SP-3	2.83	0.95	0.42	0.05	1.078	0.50
MR121-SP-4	2.86	0.95	0.40	0.05	1.107	0.54
MR121-SP-5	2.76	0.97	0.35	0.03	1.051	0.63
MR121-SP-6	2.89	0.98	0.31	0.02	1.134	0.89
MR121-SP-1-TTT	2.02	0.49	0.38	0.51	1.064	0.10
MR121-SP-1-GGG	2.18	0.48	0.42	0.52	1.182	0.10
MR121-SP-1*-TTT	2.23	0.77	0.35	0.23	1.202	0.06
MR121-SP-1** <sup>7</sup> -TTT	1.93	0.86	0.30	0.14	1.189	0.04

Fluorescence lifetimes of 10<sup>-7</sup> M solutions of DNA-hairpins were measured at the emission maxima. Relative fluorescence quantum yields were determined with respect to the free dye under similar experimental conditions (error from three independent measurements: 10% for  $\Phi_{f,rel}$ ).

from 0.43 for MR121-SP-2 to 0.63 for MR121-SP-5. Computational calculations of the donor properties of guanine in respect to neighboring bases indicate that the ionization potential of guanine is lowered substantially by neighboring purine bases, the effect being larger for guanine versus adenine and for GGG versus GG and a single G.<sup>48,49</sup> This is reflected in the different fluorescence quantum yields of MR121-SP-2 ( $\Phi_{f,rel} = 0.43$ ) carrying only a single guanosine residue and MR121-SP-1 ( $\Phi_f = 0.20$ ) with four guanosine residues in the complementary stem.

Experiments addressing electron transfer through DNA using attached donors and acceptors have provided remarkably different assessments of the electronic coupling provided by DNA.<sup>34,35,42,43,50-52</sup> Values for  $\beta$ , the decay of electronic coupling with distance, ranging from <0.1 to 1.4 Å<sup>-1</sup> have been reported. Using intercalating or well-stacked probes, electron-transfer reactions proceed on a fast time scale and exhibit shallow distance dependence (<0.1-0.4 Å<sup>-1</sup>). Here, the quenching efficiency strongly depends on stacking quality; in the presence of base mismatches or other stacking perturbations, long-range ET is essentially turned off.<sup>51,52</sup> Donors or acceptors interacting with the DNA base stack through  $\sigma$ -linkages or limited stacking have revealed much slower electron-transfer kinetics and steeper distance dependences.<sup>50,53</sup>

The multiexponential fluorescence decays observed in the MR121 labeled DNA-hairpins with an unresolved component with a decay time shorter than ~40 ps does not permit measurements of charge separation rates on the basis of TCSPC data. Therefore, relative fluorescence quantum yields obtained from steady-state measurements were used to evaluate the

distance dependence of charge-separation efficiency. The steady-state quenching yield exhibits a logarithmic dependence on the distance separating the oxazine derivative and the guanosine residue in the double-stranded stem (Figure 5C). Qualitatively, it is apparent that the double-stranded stem facilitates efficient electron transfer from the guanosine residue to MR121 with a shallow distance dependence ( $\beta = 0.1$  Å<sup>-1</sup> obtained from slope of the line in Figure 5C). Nevertheless, a meaningful value of  $\beta$  cannot be extracted from these data because of the fast time scale of electron transfer at all of the donor/acceptor distances investigated.

**Optimization of the Quenching Efficiency in DNA-Hairpins.** Overall, these considerations suggest that the oxazine derivative MR121 is associated with the terminal base pair of the DNA-hairpin stem primarily because of stabilizing hydrophobic interactions. These stacking complexes are responsible for ultrafast fluorescence quenching. Similar end-capped conformations were suggested for double-stranded oligonucleotides labeled at the 5'-terminus with anthraquinone<sup>54</sup> and Cy3.<sup>55</sup> Furthermore, we investigated the influence of single-strand overhanging nucleotides at the 3'-terminus of the DNA-hairpin on the quenching efficiency. As can be seen in Table 4, both DNA-hairpins, MR121-SP-1-TTT and MR121-SP-1-GGG, exhibit a relative fluorescence quantum yield,  $\Phi_{f,rel}$ , of 0.10. That is, the overall observed quenching efficiency is substantially higher compared to the DNA-hairpin without the single-stranded overhang (MR121-SP-1). The strong increase in the amplitude of the short fluorescence decay component,  $\tau_2$ , demonstrates that a bigger portion of the quenching proceeds on a measurable time scale, that is, >~40 ps. Nevertheless, the overall quenching efficiency can be duplicated by the simple attachment of both, additional single-stranded purine or pyrimidine nucleotides, at the 3'-terminus. On one hand, overhanging nucleotides have an influence on the interaction geometry within the end-capped conformation. If coplanar stacking is constrained only slightly, quenching with ultrafast fluorescence decay times might be reduced. On the other hand, the additional single-stranded nucleotides might stabilize the stacking interactions in the end-capped conformation thus increasing the overall quenching efficiency. To further optimize the quenching efficiency in these DNA-hairpin systems, guanosine residues were partly exchanged by 7-deazaguanosine (G<sup>7</sup>). As expected, for a stronger electron donor with an oxidation potential of ~1.00 V versus SCE,<sup>42,43</sup> the relative fluorescence quantum yield,  $\Phi_{f,rel}$ , decreases to 0.06 and 0.04 for one G<sup>7</sup> and two G<sup>7</sup> residues, respectively (Table 4). These results demonstrate the possibility to synthesize DNA-hairpins solely quenched by guanosine residues and its analogues with a more than 20-fold increase in fluorescence intensity upon specific binding to the target sequence.

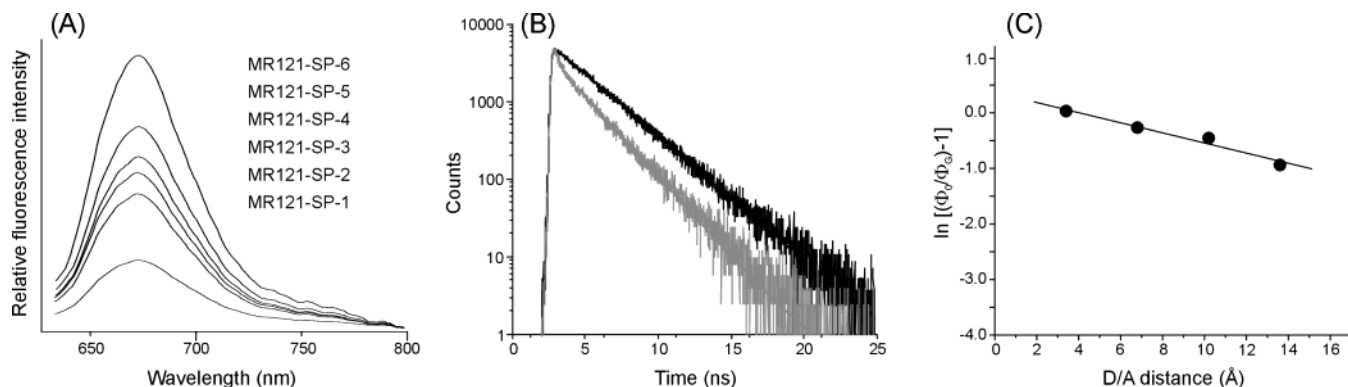


**Figure 5.** (A) Fluorescence emission spectra of different MR121 labeled DNA-hairpins ( $10^{-7}$  M) in PBS buffer, pH 7.4, containing 5 mM  $\text{MgCl}_2$ . (B) Fluorescence decay curves of MR121-SP-6 with a relative fluorescence quantum yield of 0.89 (black) and MR121-SP-1 with  $\Phi_{f,\text{rel}} = 0.20$  (gray) monitored at 680 nm in PBS buffer, pH 7.4, containing 5 mM  $\text{MgCl}_2$ . Excitation of the samples was performed at 635 nm (5000 photon counts in maximum channel, 2048 channels). (C) Distance dependence of steady-state fluorescence quenching in DNA-hairpins containing a single guanosine residue in the stem. Data shown are for MR121-SP-2, MR121-SP-3, MR121-SP-4, and MR121-SP-5.

The idea of an end-capped conformation of MR121 on the double-stranded stem of the DNA-hairpin is further supported by fluorescence anisotropy measurements which demonstrate that MR121 cannot be regarded as a free rotor. For MR121 labeled DNA-hairpins, steady-state fluorescence anisotropy values in the range of 0.30–0.38 were measured, indicating that the movement of the fluorophore is extremely constrained by the DNA independent of the sequence. Closer examination of the anisotropy values for MR121 shows that the anisotropy is slightly higher in DNA-hairpins carrying additional overhanging single-stranded bases at the 3'-end. MR121 is positively charged and so could be held on the end of the duplex in an end-capped conformation by a combination of hydrophobic and attractive electrostatic forces. A relatively fixed location in an end-capped conformation with nearly coplanar orientation of the oxazine chromophore and the DNA bases is consistent with the high anisotropy of MR121 and the strong fluorescence quenching by guanosine residues and its derivatives with shallow distance dependence. As the dynamical nature of the DNA base stack gives rise to a distribution of conformations, only a fraction of the population will take an end-capped conformation with ultrafast electron transfer. All these conformations vary with time as a result of the dynamical motions within DNA, which occur on picosecond to millisecond time scales.<sup>56,57</sup> For DNA-hairpins that contain certain defects, for example, transiently destacked base pairs, coupling is reduced to such an extent that electron transfer becomes impossible during the lifetime of the excited singlet state. These inactive structures contribute to the observed long fluorescence decay components with lifetimes  $>2$  ns. In addition, the molecular structure of the chromophore has an important influence on the stacking efficiency. For the R6G labeled DNA-hairpin R6G-SP-1, coplanar stacking of the rhodamine chromophore is constrained by the carboxyphenyl ring which is oriented nearly perpendicular to the chromophore. Therefore, electron transfer takes place on a slower time scale with fluorescence lifetimes that completely account for the quenching observed in steady-state experiments (Table 4). In contrast, because of the symmetrical planar structure, MR121 can adopt end-capped conformations which are active for fast charge separation. The fact that the overall quenching efficiency is substantially lower for JA242 labeled DNA-hairpins ( $\Phi_{f,\text{rel}} = 0.44$ ) can be explained by the three additional methyl groups (Figure 2) which certainly impede coplanar stacking in an end-capped conformation and therefore reduce the amount of ultrafast quenching.

## Conclusions

We have studied the inter- and intramolecular quenching efficiency of DNA nucleotides with rhodamine and oxazine derivatives in aqueous solution. Our results show that similar to the aggregation tendency of organic dyes, oxazine and rhodamine dyes tend to aggregate with DNA nucleotides in aqueous surroundings. The formation of ground-state complexes is reflected by shifts in the absorption and emission maxima. The extent of aggregation is controlled by the hydrophobicity of the dye. In case of aggregation with guanosine, the resulting quenching via photoinduced electron transfer is controlled by steric requirements of the dye structure and the redox properties. The bimolecular quenching constants point out that efficient quenching occurs only in these complexes, that is, at van der Waals contact ( $\sim 0.4$  nm). Furthermore, this strong static quenching is not reflected in a reduction of the fluorescence lifetimes, especially for the two oxazine derivatives. This implies that dependent on the relative conformations and resulting interaction geometries the complexes can be considered as essentially nonfluorescent. Among the four dyes investigated, R6G exhibits the highest association constant of  $K_{\text{as}} = 182 \text{ M}^{-1}$  with dGMP, and the oxazine derivative MR121 exhibits the most pronounced quenching efficiency. Our intramolecular quenching experiments using model DNA-hairpins with guanosine residues in the complementary stem demonstrate that the oxazine derivative MR121 is strongest quenched with a shallow distance dependence, that is, the double-stranded stem of the hairpin facilitates efficient electron transfer from the guanosine residue to the end-capped oxazine derivative. An end-capped conformation with nearly coplanar orientation of the oxazine chromophore and the DNA bases is consistent with the high anisotropy values measured for MR121 labeled hairpins. Furthermore, our data show that quenching of 5'-labeled DNA-hairpins can be increased substantially by the attachment of overhanging nucleotides or the exchange of guanosine by 7-deazaguanosine with a lower oxidation potential. The results obtained demonstrate that a careful selection of fluorescent dyes in relation to molecular structure and redox properties enable the synthesis of DNA-hairpins solely quenched by guanosine residues and its analogues with a 20-fold increase in fluorescence intensity upon specific binding to the target sequence. Because the use of DNA-hairpins in terms of molecular beacons becomes increasingly important in various *in vitro* and *in vivo* DNA or RNA detection methods, nucleobase-specific fluorescence quenching of dyes cannot be neglected. It is apparent that dependent

on the dyes used in donor/acceptor labeled molecular beacons the observed fluorescence quenching in the closed state is influenced by nucleobase-specific quenching interactions and cannot be ascribed purely to the desired energy transfer between the donor and acceptor dye.

**Acknowledgment.** We thank Prof. K. H. Drexhage (Universität-Gesamthochschule Siegen) for providing the oxazine derivatives MR121 and JA242. This work was supported by the BMBF (Grants 311864 and 13N8349).

## References and Notes

- Cardullo, R. A.; Agrawal, S.; Flores, C.; Zamecnik, P. C.; Wolf, D. E. *Proc. Natl. Acad. Sci. U.S.A.* **1988**, *85*, 8790.
- Parkhurst, K. M.; Parkhurst, L. J. *Biochemistry* **1995**, *34*, 285.
- Millar, D. P. *Curr. Opin. Struct. Biol.* **1996**, *6*, 322.
- Glazer, A. N.; Mathies, R. A. *Curr. Opin. Biotech.* **1997**, *8*, 94–102.
- Heid, C. A.; Stevens, J.; Livak, K. J.; Williams, P. M. *Genome Res.* **1996**, *6*, 986.
- Whitcombe, D.; Theaker, J.; Guy, S. P.; Brown, T.; Little, S. *Nature Biotech.* **1999**, *17*, 804.
- Förster, Th. *Annalen der Physik* **1948**, *2*, 55.
- Clegg, R. M.; Murchie, A. I. H.; Zechel, A.; Carlberg, C.; Diekmann, S.; Lilley, D. M. J. *Biochemistry* **1992**, *31*, 4846.
- Speiser, S. *Chem. Rev.* **1996**, *96*, 1953.
- Tyagi, S.; Kramer, F. R. *Nature Biotech.* **1996**, *14*, 303.
- Tyagi, S.; Bratu, D.; Kramer, F. R. *Nature Biotech.* **1998**, *16*, 49.
- Kostrikis, L. G.; Tyagi, S.; Mhlanga, M. M.; Ho, D. D.; Kramer, F. R. *Science* **1998**, *279*, 1228.
- Fang, X.; Liu, X.; Schuster, S.; Tan, W. *J. Am. Chem. Soc.* **1999**, *121*, 2921.
- Neuweiler, H.; Schulz, A.; Vaiana, A. C.; Smith, J. C.; Kaul, S.; Wolfrum, J.; Sauer, M. *Angew. Chem., Int. Ed.* **2002**, *41*, 4769.
- Sauer, M. *Angew. Chem., Int. Ed.* **2003**, *115*, 1790.
- Edman, L.; Mets, Ü.; Rigler, R. *Proc. Natl. Acad. Sci. U.S.A.* **1996**, *93*, 6710.
- Eggeling, C.; Fries, J. R.; Brand, L.; Gunther, R. Seidel, C. A. M. *Proc. Natl. Acad. Sci. U.S.A.* **1998**, *95*, 1556.
- Widengren, J.; Dapprich, J.; Rigler, R. *Chem. Phys.* **1997**, *216*, 417.
- Sauer, M.; Drexhage, K. H.; Lieberwirth, U.; Müller, R.; Nord, S.; Zander, C. *Chem. Phys. Lett.* **1998**, *284*, 153.
- Nazarenko, I.; Lowe, B.; Darfler, M.; Ikonomi, P.; Schuster, D.; Rashtchian, A. *Nucleic Acids Res.* **2002**, *30*, e37.
- Nazarenko, I.; Pires, R.; Lowe, B.; Obaidy, M.; Rashtchian, A. *Nucleic Acids Res.* **2002**, *30*, 2089.
- Kurata, S.; Kanagawa, T.; Yamada, K.; Torimura, M.; Yokomaku, T.; Kamagata, Y.; Kurane, R. *Nucleic Acids Res.* **2001**, *29*, e34.
- Lianos, P.; Georghiou, S. *Photochem. Photobiol.* **1979**, *29*, 13.
- Shafirovich, V. Y.; Courtney, S. H.; Ya, N.; Geacintov, N. E. *J. Am. Chem. Soc.* **1995**, *117*, 4920.
- Lewis, F. D.; Letsinger, R. L.; Wasielewski, M. R. *Acc. Chem. Res.* **2001**, *34*, 159.
- Seidel, C. A. M.; Schulz, A.; Sauer, M. *J. Phys. Chem.* **1996**, *100*, 5541.
- Knemeyer, J. P.; Marmé, N.; Sauer, M. *Anal. Chem.* **2000**, *72*, 3717.
- Steenken, S.; Jovanovic, V. *J. Am. Chem. Soc.* **1997**, *119*, 617.
- Piestert, O.; Barsch, H.; Buschmann, V.; Heinlein, T.; Knemeyer, J. P.; Weston, K. D.; Sauer, M. *Nano Lett.* **2003**, ASAP.
- Lee, S.; Winnik, M. A. *Macromolecules* **1997**, *30*, 2633.
- Daugherty, D. L.; Gellman, S. H. *J. Am. Chem. Soc.* **1999**, *121*, 4325.
- Zhong, D.; Zewail, A. H. *Proc. Natl. Acad. Sci. U.S.A.* **2001**, *98*, 11867.
- Malaga, N.; Chosrowjan, H.; Shibata, Y.; Tanaka, F.; Nishina, Y.; Shiga, K. *J. Phys. Chem. B* **2000**, *104*, 10667.
- Lewis, F. D.; Wu, T.; Zhang, Y.; Letsinger, R. L.; Greenfield, S. R.; Wasielewski, M. R. *Science* **1997**, *277*, 673.
- Lewis, F. D.; Letsinger, R. L.; Wasielewski, M. R. *Acc. Chem. Res.* **2001**, *34*, 159.
- Rehm, D.; Weller, A. *Isr. J. Chem.* **1970**, *8*, 259.
- Marcus, R. A.; Sutin, N. *Biochim. Biophys. Acta* **1985**, *811*, 265.
- Jones L. G.; Lu, L. N.; Fu, H.; Farahat, C. W.; Oh, C.; Greenfield, S. R.; Gosztola, D. J.; Wasielewski, M. R. *J. Phys. Chem. B* **1999**, *103*, 572.
- Weller, A. *Z. Phys. Chem. Neue Folg.* **1982**, *133*, 93.
- Wagenknecht, H. A.; Stemp, E. D. A.; Barton, J. K. *J. Am. Chem. Soc.* **2000**, *122*, 1.
- DeFelippis, M. R.; Murthy, C. P.; Broitman, F.; Weinraub, D.; Faraggi, M.; Klapper, M. H. *J. Phys. Chem.* **1991**, *95*, 3416–3419.
- Fiebig, T.; Wan, C.; Kelley, S. O.; Barton, J. K.; Zewail, A. H. *Proc. Natl. Acad. Sci. U.S.A.* **1999**, *96*, 1187.
- Wan, C.; Fiebig, T.; Kelley, S. O.; Treadway, C. R.; Barton, J. K.; Zewail, A. H. *Proc. Natl. Acad. Sci. U.S.A.* **1999**, *96*, 6014.
- Dietrich, A.; Buschmann, V.; Müller, C.; Sauer, M. *Rev. Mol. Biotechnol.* **2002**, *82*, 211.
- Sauer, M.; Han, K. T.; Müller, R.; Nord, S.; Schulz, A.; Seeger, S.; Wolfrum, J.; Arden-Jacob, J.; Deltau, G.; Marx, N. J.; Zander, C.; Drexhage, K. H. *J. Fluoresc.* **1995**, *5*, 247.
- Sauer, M.; Drexhage, K. H.; Herten, D. P.; Lieberwirth, U.; Müller, R.; Neumann, M.; Nord, S.; Siebert, S.; Schulz, A.; Zander, C.; Wolfrum, J. In *Near-Infrared Dyes for High Technology Applications*; Daehne, S., Ed.; Kluwer: Dordrecht, The Netherlands, 1998; pp 57–85.
- Neuweiler, H.; Schulz, A.; Böhmer, M.; Enderlein, J.; Sauer, M. *J. Am. Chem. Soc.* **2003**, *125*, 5324.
- Sugiyama, H.; Saito, I. *J. Am. Chem. Soc.* **1996**, *118*, 7063.
- Prat, F.; Houk, K. N.; Foote, C. S. *J. Am. Chem. Soc.* **1998**, *120*, 845.
- Meade, T. J.; Kayyem, J. F. *Angew. Chem., Int. Ed. Engl.* **1995**, *34*, 352.
- Kelley, S. O.; Holmlin, R. E.; Stemp, E. D. A.; Barton, J. K. *J. Am. Chem. Soc.* **1997**, *119*, 9861.
- Kelley, S. O.; Barton, J. K. *Science* **1999**, *283*, 375.
- Fukui, K.; Tanaka, K. *Science* **1999**, *283*, 158.
- Kan, Y.; Schuster, G. B. *J. Am. Chem. Soc.* **1999**, *121*, 10857.
- Norman, D. G.; Grainger, R. J.; Uhrin, D.; Lilley, D. M. J. *Biochemistry* **2000**, *39*, 6317.
- Robinson, B. H.; Mailer, C.; Drobny, G. *Annu. Rev. Biophys. Biomol. Struct.* **1997**, *26*, 629.
- Wallace, M. I.; Ying, L. M.; Balasubramanian, S.; Klenerman, D. *Proc. Natl. Acad. Sci. U.S.A.* **2001**, *98*, 5584.